DEVELOPMENT OF OBSTACLE AVOIDANCE SYSTEM USING CO-OPERATIVE CONTROL

Yukihiro Fujiwara * **Yasushi Shoda** * **Shuichi Adachi** **

* *Honda R&D Co., Ltd., 4630 Shimotakanezawa, Haga-machi, Haga-gun, Tochigi, Japan*
** *Utsunomiya University, 7-1-2 Yoto, Utsunomiya, Tochigi, Japan*

Abstract: This paper proposes a new driver support system which assists driver's operation in an obstacle avoidance scene. The proposed system has actuator systems which are Electric Power Steering (EPS) and Direct Yaw-moment Control (DYC). The obstacle is detected as a differential feature value by using a micro-wave radar instead of a camera. Co-operative control is constructed to manage the actuators by frequency weighting functions. By experiments using an actual vehicle, it is shown that the proposed system has effectiveness for assistance the driver's operation for an avoidance task and for improving vehicle dynamics. *Copyright©2005 IFAC*

Keywords: Co-operative control, Vehicle dynamics, Automotive control

1. INTRODUCTION

The prevention of traffic accidents is one of social requests. Systems which prevent the accidents have been developed by a variety of schemes, for example, by adding some intelligence to a vehicles (T.Miyazaki, 1997). As an intelligent vehicle, driver support systems (M.Ikegaya and S.Kondo, 1998), which has an outfield sensor such as a camera and a radar installed in the vehicle, have been investigated.

On the other hand, in research area of vehicle dynamics control, Direct Yaw-Moment Control (DYC) (M.Abe, 1998) and a vehicle control system (M.Shino and M.Nagai, 1998), which is integrated by DYC and active front steering system (AFS), are proposed to improve active safety performance of the vehicle.

In such a background, by fusion of outfield sensor technology and of vehicle dynamics control technology, a system that supports driver's operation during evasive lane change is proposed(Y.Furukawa and B.Y.Wang, 2002). A problem of this system is how to describe outfield sensor signal as the vehicle control signal because this signal influences performance of the driver support systems.

Authors proposed a method called visual feedback structure to describe the outfield sensor signal in past study (T.Komori and K.Uchida, 2000). In this method, a preview road shape and an obstacle were defined as a feature value on a virtual camera image. The method, however, had a problem which it was difficult to detect the feature value with an actual camera.

This paper proposes a control system design method of the driver support system which assists driver's operation in an obstacle avoidance scene called double lane change maneuver. In this design method, a differential signal of the feature value is used as the control signal and it is indicated that the differential feature value is detected with an actual radar sensor instead of the camera.

This system has a steering actuator such as Electric Powered Steering (EPS) and a brake actuator to realize DYC function. Characteristics of

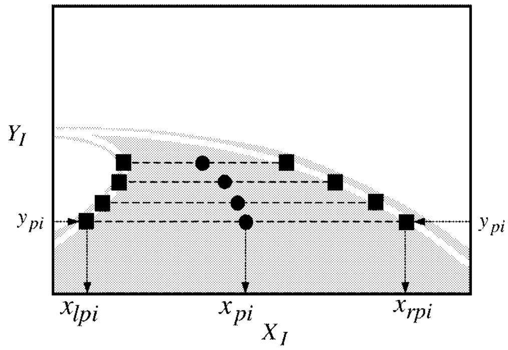

Fig. 1. Forward image with feature points.

the actuators are described as frequency weighting functions which depend on characteristics of each actuators. A co-operative controller is designed by Linear Quadratic Integration (LQI) method considered with the weighting functions. It is shown that the proposed system has performance for improving the vehicle dynamics and for compensating driver's operation by the vehicle testing called double lane change maneuver.

2. SYSTEM CONFIGURATION

2.1 Driving scene

Fig.1 shows the preview road shape. By setting up feature points (x_{lpi}, x_{rpi}, x_{pi}), the road shape called the feature value is described as,

$$\tilde{X}_{sum} = \sum_{i=1}^{n} a_i x_{pi}, \quad (1)$$

where a_i are design parameters.

In a case to avoid the obstacle, recognition of the feature value is shown as Fig.2 (Y.Fujiwara and S.Adachi, 2004). The feature value to avoid the obstacle is described as,

$$X_{sum} = \tilde{X}_{sum} + \sum_{i=1}^{n} a_i \Delta x_{pi}, \quad (2)$$

because the obstacle is considered as a disturbance signal.

In order to analyze behavior of the feature value, X_{sum}, eq.(2) is differentiated with respect to time. Then,

$$\begin{aligned} \dot{X}_{sum} &= \sum_{i=1}^{n} a_i \dot{x}_{pi} \\ &= \sum_{i=1}^{n} a_i \left(\frac{f}{\lambda} \dot{\theta}_y - \frac{y_{pi}}{H} V_x + \frac{y_{pi}}{H} T_{xi} \right), \quad (3) \end{aligned}$$

where f and λ are focal length of the camera lens and length of a pixel, respectively. H, θ_y, V_x, and

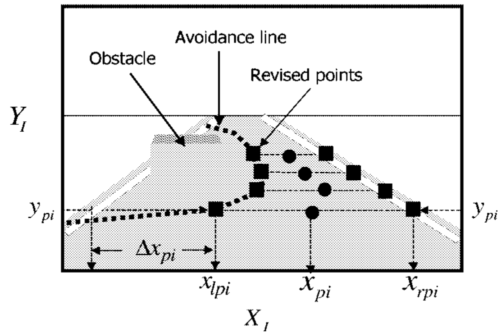

Fig. 2. Forward image with feature points (obstacle avoidance scene).

T_{xi} are the height at which the camera is installed, a rotational angle of the camera, the velocity of the camera to lateral direction, and the variation of feature points for the road shape, respectively. A differential value of the disturbance signal is defined as,

$$\Delta \dot{x}_{pi} = 0. \quad (4)$$

If the road shape does not change,

$$T_{xi} = -V \sin \theta_y \quad (5)$$

is obtained, where V is the vehicle speed.

2.2 Vehicle dynamics

In general, vehicle movement is a 6-degree-of-freedom system. However, the vehicle model is constructed only for lateral axis motion caused by steering operation. Therefore, as shown in Fig.3, vehicle motion is described by rotational motion yaw-rate γ around an axis which is orthogonal to $X_v - Z_v$ plane Σ_v and by side slip angle β which depends on the vehicle motion on the X_v-axis. This approximation enables the vehicle model to be described as

$$\dot{x}_v = A_v x_v(V) + B_{v1}(V)\theta_f^R + B_{v2}M, \quad (6)$$

which is a 2-degree-of-freedom model, where

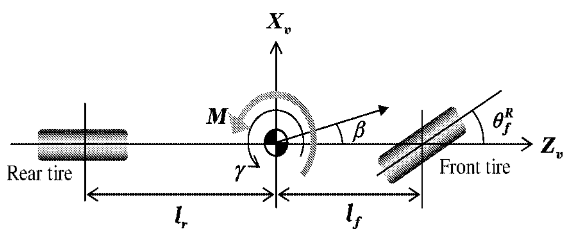

Fig. 3. Two wheels vehicle model.

$$
\mathsf{x}_{\mathsf{v}} = \begin{bmatrix} \gamma \\ \beta \end{bmatrix},
$$

$$
\mathsf{A}_{\mathsf{v}}(V) = \begin{bmatrix} \dfrac{-2(K_{\mathsf{f}} l_{\mathsf{f}}^2 + K_{\mathsf{r}} l_{\mathsf{r}}^2)}{I_{\mathsf{y}} V} & \dfrac{-2(K_{\mathsf{f}} l_{\mathsf{f}} - K_{\mathsf{r}} l_{\mathsf{r}})}{I_{\mathsf{y}}} \\ \dfrac{-2(K_{\mathsf{f}} l_{\mathsf{f}} - K_{\mathsf{r}} l_{\mathsf{r}})}{m V^2} - 1 & \dfrac{-2(K_{\mathsf{f}} + K_{\mathsf{r}})}{m V} \end{bmatrix},
$$

$$
\mathsf{B}_{\mathsf{v1}}(V) = \begin{bmatrix} \dfrac{2K_{\mathsf{f}} l_{\mathsf{f}}}{I_{\mathsf{y}}} \\ \dfrac{2K_{\mathsf{f}}}{mV} \end{bmatrix}, \quad \mathsf{B}_{\mathsf{v2}} = \begin{bmatrix} \dfrac{1}{I_{\mathsf{y}}} \\ 0 \end{bmatrix},
$$

where l_{f} is distance between the center of gravity (C.G.) and the front axle, l_{r} is distance between the C.G. and the rear axle, K_{f} is the cornering power of a front tire, K_{r} is the cornering power of a rear tire, I_{y} is the yaw inertia moment, m is the vehicle weight, and $\theta_{\mathsf{f}}^{\mathsf{R}}$ is the front wheel angle and M is yaw-moment.

2.3 Integrating driving scene and vehicle dynamics

If the camera is fixed to the vehicle, then

$$
\dot{\theta}_{\mathsf{y}} = \gamma \tag{7}
$$

$$
V_{\mathsf{x}} = V\beta \tag{8}
$$

are obtained. A mathematical model integrated the driving scene and vehicle dynamics are described by (3) and (6).

$$
\dot{\mathsf{x}}_{\mathsf{p}} = \mathsf{A}_{\mathsf{p}}(V)\mathsf{x}_{\mathsf{p}} + \mathsf{B}_{\mathsf{p1}}(V)\theta_{\mathsf{f}}^{\mathsf{R}} + \mathsf{B}_{\mathsf{p2}} M + \mathsf{d}_{\mathsf{w}} w_{\mathsf{t}} \tag{9}
$$

$$
X_{\mathsf{sum}} = \mathsf{C}_{\mathsf{p}} \mathsf{x}_{\mathsf{p}} + \sum_{\mathsf{i}=1}^{\mathsf{n}} \mathsf{a}_{\mathsf{i}} \Delta \mathsf{x}_{\mathsf{pi}}, \tag{10}
$$

where

$$
\mathsf{A}_{\mathsf{p}}(V) = \begin{bmatrix} \dfrac{-2(K_{\mathsf{f}} l_{\mathsf{f}}^2 + K_{\mathsf{r}} l_{\mathsf{r}}^2)}{I_{\mathsf{y}} V} & \dfrac{-2(K_{\mathsf{f}} l_{\mathsf{f}} - K_{\mathsf{r}} l_{\mathsf{r}})}{I_{\mathsf{y}}} & 0 \\ \dfrac{-2(K_{\mathsf{f}} l_{\mathsf{f}} - K_{\mathsf{r}} l_{\mathsf{r}})}{m V^2} - 1 & \dfrac{-2(K_{\mathsf{f}} + K_{\mathsf{r}})}{m V} & 0 \\ \dfrac{f}{\lambda} \Sigma_{\mathsf{i}=1}^{\mathsf{n}} a_{\mathsf{i}} & -\dfrac{V}{H} \Sigma_{\mathsf{i}=1}^{\mathsf{n}} a_{\mathsf{i}} y_{\mathsf{pi}} & 0 \end{bmatrix},
$$

$$
\mathsf{B}_{\mathsf{p1}}(V) = \begin{bmatrix} \dfrac{2K_{\mathsf{f}} L_{\mathsf{f}}}{I_{\mathsf{y}}} \\ \dfrac{2K_{\mathsf{f}}}{mV} \\ 0 \end{bmatrix}, \quad \mathsf{B}_{\mathsf{p2}} = \begin{bmatrix} \dfrac{1}{I_{\mathsf{y}}} \\ 0 \\ 0 \end{bmatrix},
$$

$$
\mathsf{C}_{\mathsf{p}} = \begin{bmatrix} 0 & 0 & 1 \end{bmatrix}, \quad \mathsf{d}_{\mathsf{w}} = \begin{bmatrix} 0 \\ 0 \\ 1 \end{bmatrix},
$$

$$
\mathsf{x}_{\mathsf{p}} = \begin{bmatrix} \gamma \\ \beta \\ X_{\mathsf{sum}} \end{bmatrix}, \quad w_{\mathsf{t}} = -\frac{V \sin\theta_{\mathsf{y}}}{H} \sum_{\mathsf{i}=1}^{\mathsf{n}} \mathsf{a}_{\mathsf{i}} \mathsf{y}_{\mathsf{pi}}.
$$

2.4 Driver's operation

An error signal $\Delta\delta_{\mathsf{f}}$ between θ_{s} called driver's operational angle and $\theta_{\mathsf{f}}^{\mathsf{R}}$ is defined by

$$
\Delta\delta_{\mathsf{f}} = \theta_{\mathsf{f}}^{\mathsf{R}} - \frac{1}{N_{\mathsf{r}}}\theta_{\mathsf{s}}, \tag{11}
$$

where N_{r} is a gear ratio between θ_{s} and $\theta_{\mathsf{f}}^{\mathsf{R}}$. Equation (11) is described as

$$
\theta_{\mathsf{f}}^{\mathsf{R}} = \frac{1}{N_{\mathsf{r}}}\theta_{\mathsf{s}} + \Delta\delta_{\mathsf{f}}. \tag{12}
$$

Then, by (9) and (12)

$$
\dot{\mathsf{x}}_{\mathsf{p}} = \mathsf{A}_{\mathsf{p}}(V)\mathsf{x}_{\mathsf{p}} + \mathsf{B}_{\mathsf{p1}}(V)\Delta\delta_{\mathsf{f}} + \mathsf{B}_{\mathsf{p2}} M + \mathsf{d}_{\mathsf{w}} w_{\mathsf{t}} + \frac{1}{N_{\mathsf{r}}} \mathsf{B}_{\mathsf{p1}}(V)\theta_{\mathsf{s}} \tag{13}
$$

is obtained.

Equation (13) shows behavior of the system that considered the driver's operation (θ_{s}).

3. CONTROL STRATEGY

3.1 Differential feature value

A driving scene of lane following and obstacle avoidance are performed by converging X_{sum} to 0 (T.Komori and K.Uchida, 2000). However, it is expected that the operation interference occurs between the support system and driver's operation because the driver does not request to drive along a fixed traveling course in generally.

It is assumed that the driver operates so that the vehicle position is kept near to the traveling course. Thus, the support system manages to converge the differential feature value ($\dot{X}_{\mathsf{sum}}$) to 0. Then, behavior of the system is given by,

$$
\begin{cases} \dot{\mathsf{x}}_{\mathsf{v}} = \mathsf{A}_{\mathsf{v}} \mathsf{x}_{\mathsf{v}}(V) + \mathsf{B}_{\mathsf{v1}}(V)\Delta\delta_{\mathsf{f}} + \mathsf{B}_{\mathsf{v2}} M + \dfrac{1}{N_{\mathsf{r}}} \mathsf{B}_{\mathsf{v1}} \theta_{\mathsf{s}} \\ z = \dot{X}_{\mathsf{sum}} = r_{\mathsf{ref}} - y_{\mathsf{s}} \\ y_{\mathsf{s}} = \mathsf{C}_{\mathsf{v}} \mathsf{x}_{\mathsf{v}} \end{cases} \tag{14}
$$

where

$$
\mathsf{C}_{\mathsf{v}} = \begin{bmatrix} \dfrac{f}{\lambda} \Sigma_{\mathsf{i}=1}^{\mathsf{n}} a_{\mathsf{i}} & -\dfrac{V}{H} \Sigma_{\mathsf{i}=1}^{\mathsf{n}} a_{\mathsf{i}} y_{\mathsf{pi}} \end{bmatrix},
$$

$$
r_{\mathsf{ref}} = \sum_{\mathsf{i}=1}^{\mathsf{n}} a_{\mathsf{i}} \left(-\frac{y_{\mathsf{pi}}}{H} V \sin\theta_{\mathsf{y}} \right).
$$

It is assumed that yaw-rate γ is larger than side slip angle β in (14). Then, next equation is defined as

$$
\frac{f}{\lambda} \sum_{\mathsf{i}=1}^{\mathsf{n}} a_{\mathsf{i}} = 1. \tag{15}
$$

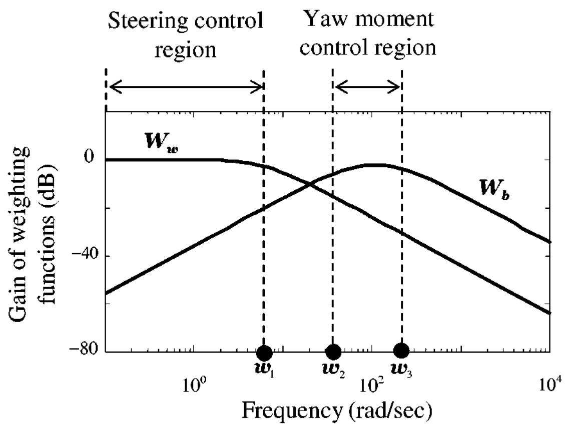

Fig. 4. Specification for actuator characteristics in frequency domain

Therefore, y_s is described as

$$y_s = \gamma. \tag{16}$$

As the result, this system makes the error signal z between the reference yaw-rate r_{ref} and the yaw-rate γ to 0.

3.2 Description of actuator characteristics

A low pass filter, which shows in Fig.4, is defined as a weighting function of EPS because operation interference with the driver occurs by driving the EPS actuator quickly. The weighting function is given by,

$$W_w : \begin{cases} \dot{x}_w &= a_w x_w + b_w u_w \\ \theta_e &= c_w x_w, \end{cases} \tag{17}$$
$$a_w = -\omega_1, \quad b_w = \omega_1, \quad c_w = 1,$$

where x_w is state variable of the weighting function W_w shown in Fig.4, u_w is a virtual input signal, ω_1 is a cut-off frequency of the W_w.

Braking force for DYC is applied between left and right tire to produce the yaw-moment M. A band pass filter is defined as a weight function W_b, because it is difficult to apply the braking force in static state.

$$W_b : \begin{cases} \dot{x}_b &= A_b x_b + B_b u_b \\ M &= C_b x_b \end{cases}, \tag{18}$$

where

$$A_b = \begin{bmatrix} 0 & 1 \\ -\omega_2\omega_3 & -(\omega_2+\omega_3) \end{bmatrix}, \quad B_b = \begin{bmatrix} 0 \\ \omega_2\omega_3 \end{bmatrix},$$
$$C_b = \begin{bmatrix} 0 & 1 \end{bmatrix},$$

u_b is a virtual input signal for the yaw-moment, ω_2 and ω_3 are cut-off frequency of the W_b.

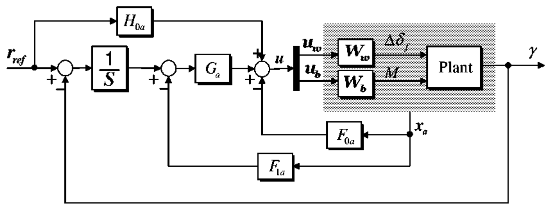

Fig. 5. Control system structure

4. DESIGN OF CO-OPERATIVE CONTROLLER

LQI is applied as controller design method because it is easy to embed the LQI controller to an Electronic Control Unit (ECU). A purpose of the co-operative control is to use the input signals selectively by frequency domain. Then, augment system for the integrated model and frequency weighting functions is given by

$$\begin{cases} \dot{x}_a &= A_a x_a + B_{a1} u_w + B_{a2} u_b + d_s \theta_s \\ y_s &= C_a x_a \end{cases} \tag{19}$$

where

$$A_a = \begin{bmatrix} A_v & B_{v1} c_w & B_{v2} C_b \\ 0 & a_w & 0 \\ 0 & 0 & A_b \end{bmatrix},$$
$$B_{a1} = \begin{bmatrix} 0 \\ b_w \\ 0 \end{bmatrix}, \quad B_{a2} = \begin{bmatrix} 0 \\ 0 \\ B_b \end{bmatrix},$$
$$C_a = \begin{bmatrix} C_v & 0 & 0 \end{bmatrix}, \quad x_a = \begin{bmatrix} \gamma & \beta & x_w & x_b \end{bmatrix}^T,$$
$$d_s = \begin{bmatrix} \frac{1}{N_r} B_{v1} & 0 & 0 \end{bmatrix}^T.$$

Fig.5 shows the control system block structure designed by the co-operative control proposed in previous section, where x_v, W_w and W_b are vehicle state variables, frequency weighting functions of steering and brake, respectively. This controller has six state variables in addition of integrator, where F_{0a} and F_{1a} are state feedback gain and feedback gain for removing integrator output, respectively. H_{0a}, G_a is feed-forward gain and integrator gain, respectively. Control inputs are steering compensated angle $\Delta\delta_f$ and yaw-moment M.

Fig.6 and Fig.7 show simulation results in step response of reference signal r_{ref}. Fig.6 shows behavior of control inputs (steering and brake) in step response of reference signal r_{ref}. Fig.7 shows effect of integrator in the similar case. The designed controller works well in low frequency domain because steady state error is zero.

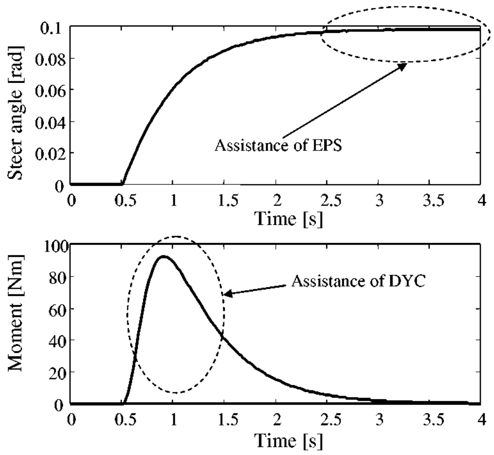

Fig. 6. Control input signals

5. RESULTS AND DISCUSSION

A compact car of 2000cc class was used as the actual vehicle, the co-operative controller descritized by 10msec was embedded to the ECU. A maneuver which recovers straight-line travel after obstacle avoidance was used. In general, this maneuver is called a double lane change maneuver shown in Fig.8.

The signal r_{ref} was measured by a micro-wave radar (no camera), because this signal is a lateral distance of the obstacle. Road friction coefficient was 0.3, the vehicle was traveling at a speed of 11m/s.

Fig.9 shows yaw-rate response and driver's steering angle for the co-operative control and without control in the double lane change maneuver. The vehicle stability was improved in region from 3sec to 5sec because almost there was not the fluctuation of yaw-rate. The driver's operational load was reduced because of decreasing revised steering to perform yaw-rate stabilization.

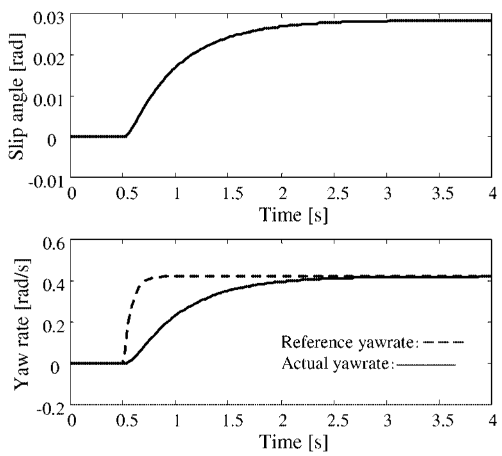

Fig. 7. Step response of slip angle and yaw-rate

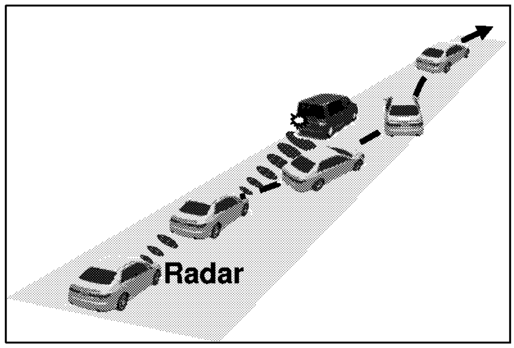

Fig. 8. Double lane change maneuver

Fig.10 shows comparison with the co-operative control and only DYC control. In term from 2.5sec to 5sec, the steering angle was small in the co-operative control. It is assumed that EPS control reduces an unnecessary steering angle.

Fig.11 shows comparison with the co-operative control and only EPS control. The co-operative control had good performance of yaw-rate convergence against only EPS control. Therefore, it is assumed that DYC control improves the vehicle dynamics.

From the results, the co-operative control integrated by DYC and EPS has the improved vehicle dynamics and supports characteristic for driver's operation during lane change maneuver.

6. CONCLUSIONS

The main results of the proposed system, which called the obstacle avoidance system, are as follows.

(1) The differential feature value which consisted of yaw-rate, side slip angle and lateral distance of the obstacle measured with the radar was used as control signal of the co-operative controller.

(2) The frequency weighting functions considered with the actuator characteristics of EPS and of DYC were used in the co-operative control design method.

(3) It was proved that the co-operative controller has been performed the improved vehicle dynamics and the assistance of the driver's operation by the actual vehicle experiment called double lane change maneuver.

REFERENCES

M.Abe, Y.Furukawa (1998). Direct yaw moment control on-board-tire-model. *Proc. of the AVEC98.*

M.Ikegaya, N.Asanuma, S.Ishida and S.Kondo (1998). Development of a lane following assistance system. *Proc. of the AVEC98.*

M.Shino, P.Raksincharoensak and M.Nagai (1998). Vehicle handling and stability control by integrated control of direct yaw moment and active steering. *Proc. of the AVEC98.*

T.Komori, Y.Fujiwara, M.Fujita and K.Uchida (2000). Automated driving by visual servoing (in japanese). *Trans. IEE of Japan.*

T.Miyazaki (1997). Plan for promotion of the development of advanced safety vehicle (asv) (in japanese). *The Journal of SICE.*

Y.Fujiwara and S.Adachi (2004). Control system design for obstacle avoidance system using model predictive control. *Proc. of the CCA.*

Y.Furukawa, M.Abe and B.Y.Wang (2002). Possibility of a driver-assist-system during evasive lane change. *Proc. of the AVEC2002.*

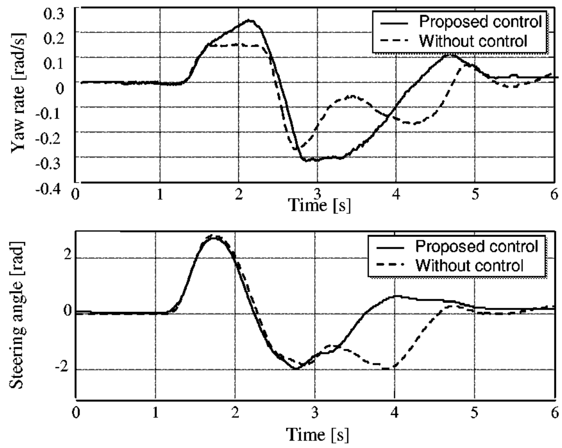

Fig. 9. Yaw-rate characteristic (co-operative control/ without control)

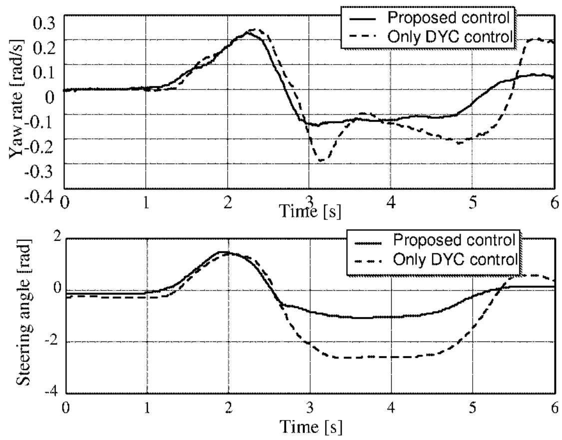

Fig. 10. Yaw-rate characteristic (co-operative control/DYC control)

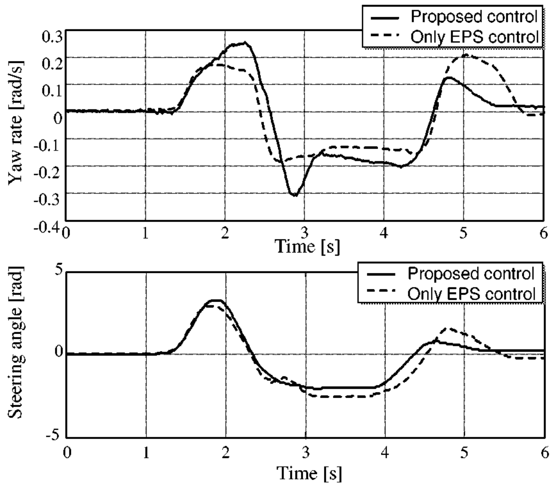

Fig. 11. Yaw-rate characteristic (co-operative control/EPS control)